JOURNAL OF COMPUTATIONAL PHYSICS 69, 434–459 (1987)

The Method of Fundamental Solutions for the Numerical Solution of the Biharmonic Equation

ANDREAS KARAGEORGHIS*

Department of Mathematics, University of Kentucky, Lexington, Kentucky 40506

AND

GRAEME FAIRWEATHER†

Departments of Mathematics and Engineering Mechanics, University of Kentucky, Lexington, Kentucky 40506

Received April 11, 1986; revised August 12, 1986

The method of fundamental solutions (MFS) is a relatively new technique for the numerical solution of certain elliptic boundary value problems. It falls in the class of methods generally called boundary methods, and, like the well-known boundary integral equation method, is applicable when a fundamental solution of the differential equation is known. In the MFS, the approximate solution is a linear combination of fundamental solutions with singularities placed outside the domain of the problem. The locations of the singularities are either preassigned or determined along with the coefficients of the fundamental solutions so that the approximate solution satisfies the boundary conditions as well as possible. In many applications, these quantities are determined by a least squares fit of the boundary conditions, a nonlinear problem, which is solved using standard software. In this paper, the MFS is formulated for biharmonic problems and is applied to a variety of standard test problems as well as to problems arising in elasticity and fluid flow. © 1987 Academic Press, Inc.

1. BACKGROUND

The two most widely used methods for the numerical solution of elliptic partial differential equations have traditionally been finite difference and finite element methods. In recent years, there has emerged a powerful alternative to these methods for the solution of certain problems, namely those for which fundamental solutions are known. Such methods are called boundary methods because, in contrast to finite difference and finite element methods, they require that only the boundary of the region of the problem be discretized, not the whole region itself. In boundary

* Present address: Department of Applied Mathematics, The University College of Wales, Penglais, Aberystwyth, Dyfed SY23 3BZ, Wales.

† Partially supported by the National Science Foundation under Grant MCS-8303287.

0021-9991/87 $3.00

Copyright © 1987 by Academic Press, Inc.
All rights of reproduction in any form reserved.

methods a first stage yields the desired numerical solution on the boundary of the region and a second stage produces approximations in the interior, if these are required. The most popular boundary methods are the boundary element methods (BEMs) or boundary integral equation methods (BIEMs) as they are sometimes called. These have proved to be so effective that they are now competing in many cases with traditional space discretization methods (see, e.g., Jaswon and Symm [18] or Banerjee and Butterfield [2]).

Some of the characteristics of BEMs can be found in all other boundary methods developed. In most of the latter, a fixed auxiliary boundary surrounding the domain of the problem is introduced, and the numerical solution is based on approximations involving points on this auxiliary boundary (see, e.g., [6, 9, 13, 24, 33, 40]).

A boundary method which is different from auxiliary boundary methods is the method of fundamental solutions (MFS), which was first proposed by Kupradze (see [1, 25, 26, 27]). In Section 2, we extend the MFS formulation of Mathon and Johnston [31], which has been succesfully applied to a variety of problems, [11, 14, 19, 28]. The MFS as implemented by these authors is, in a sense, a generalization of auxiliary boundary methods, as points determining an auxiliary boundary surrounding the region are allowed to move freely and their coordinates are variables in a minimization problem. Other MFS-type formulations are discussed in [5, 6, 7, 22, 44, 45].

2. Boundary Methods for the Solution of the Biharmonic Equation

In many cases, boundary methods have been used for the numerical solution of the biharmonic equation, which occurs in the theory of thin plates and slow flow problems. Indirect BEMs were first used by Jaswon, Maiti, and Symm [16], Jaswon and Maiti [17], and Maiti and Chakrabarti [29], but these methods seemed to be ill-conditioned for certain boundary conditions in cases when the region under consideration included corners. Segedin and Brickell [35] were the first to use a direct BEM for the solution of biharmonic problems. Their results were satisfactory, but restricted to simply supported plates. A general formulation of a direct BEM was first suggested by Fairweather *et al.* [10], and this was applied recently by Kelmanson [22, 23] to a variety of biharmonic problems which involve boundary singularities. Kelmanson also developed a modified BEM incorporating a subtraction of singularity technique (cf. [37]), and this procedure produced very satisfactory results. Other BEM approaches have been proposed in [3, 4, 8, 12, 34, 36, 39, 41, 42, 43, 46]. MFS-type methods for the solution of the biharmonic equation were used by Murashima, Nonaka, and Nieda [32] for plate bending problems, and by Burgess and Mahajerin [7] for a slow flow problem, and by Bogomolny [5], who examined mathematical aspects of MFS formulations for the solution of various elliptic boundary value problems, and presented several numerical examples.

3. The Biharmonic MFS (BMFS)

We consider the biharmonic equation

$$\nabla^2(\nabla^2\psi(p)) = \nabla^4\psi(p) = 0 \tag{1}$$

in a closed, bounded domain Ω in the plane, subject to either

(i)
$$B_1\psi(p) \equiv \alpha(p) + \psi(p) = 0,$$
$$B_2\psi(p) \equiv \beta(p) + \frac{\partial\psi(p)}{\partial n} = 0, \qquad \text{for} \quad p \in \partial\Omega,$$

or

(ii)
$$B_1\psi(p) \equiv \alpha(p) + \psi(p) = 0,$$
$$B_2\psi(p) \equiv \beta(p) + \nabla^2\psi(p) = 0, \qquad \text{for} \quad p \in \partial\Omega.$$

As in [5] and [32], we consider a BMFS approximation of the form:

$$\psi_N(c, d, t, p_i) = \sum_{j=1}^{N} c_j K_1(t_j, p_i) + \sum_{j=1}^{N} d_j K_2(t_j, p_i), \tag{2}$$

where

$$c = [c_1, c_2, c_3, \ldots, c_N]^T,$$
$$d = [d_1, d_2, d_3, \ldots, d_N]^T,$$
$$t = [t_{1_1}, t_{1_2}, t_{2_1}, t_{2_2}, t_{3_1}, t_{3_2}, \ldots, t_{N_1}, t_{N_2}]^T,$$

(t_{j_1}, t_{j_2}) are the coordinates of the singularity t_j, a point outside $\bar{\Omega}$, (p_{i_1}, p_{i_2}) are the coordinates of the point p_i, where $p_i \in \bar{\Omega}$,

$$r_{ji} = \sqrt{(t_{j_1} - p_{i_1})^2 + (t_{j_2} - p_{i_2})^2}$$

and

$$K_1(t_j, p_i) = r_{ji}^2 \log(r_{ji}),$$
$$K_2(t_j, p_i) = \log(r_{ji}). \tag{3}$$

That is, we approximate the solution to the biharmonic problem by a linear combination of fundamental solutions of both the biharmonic equation and Laplace's equation. Clearly the approximation (2) satisfies the biharmonic equation. The next step is to determine coefficients c_j and d_j, and locations of the singularities t_j for which the approximation (2) satisfies the boundary conditions as well as possible.

This is done by choosing M points p_i on the boundary $\partial\Omega$ and minimizing the functional

$$F(c, d, t) = \sum_{i=1}^{M} \{|B_1\psi_N(p_i)|^2 + |B_2\psi_N(p_i)|^2\} \tag{4}$$

which is nonlinear in the t_j's (cf. [31]). The minimization of this functional is done using a nonlinear least squares algorithm. The number M of boundary points is chosen to be approximately three times the number of unknowns, that is $M \approx 12 \cdot N$, as four unknowns correspond to each singularity.

To improve the rate of convergence of the least squares algorithm, instead of using the expressions (3) for $K_1(t_j, p_i)$ and $K_2(t_j, p_i)$, we use the normalized fundamental solutions:

$$\begin{aligned} K_1(t_j, p_i) &= \left(\frac{r_{ji}}{\rho + \sqrt{t_{j1}^2 + t_{j2}^2}}\right)^2 \log\left(\frac{r_{ji}}{\rho + \sqrt{t_{j1}^2 + t_{j2}^2}}\right)^2 \\ K_2(t_j, p_i) &= \log\left(\frac{r_{ji}}{\rho + \sqrt{t_{j1}^2 + t_{j2}^2}}\right)^2 \end{aligned} \tag{5}$$

where ρ is usually taken to be the radius of a circle containing the region under consideration.

A factor of great importance in the least squares procedure is the initial placement of the singularities. In most of the problems considered, it was observed that distributing the singularities uniformly around the region was a good general rule, as this produced satisfactory results. The singularities were placed along the normals to the surface, at chosen boundary points, at a fixed distance from the boundary, as described in [14] (see Fig. 1). In most cases, the distance was taken to be 0.1.

Since the minimization routine requires starting values for all the variables, the coefficients c_j and d_j were initially chosen to be equal to 1. Further, the boundary points were, in most cases, spread uniformly around the boundary.

The least squares algorithms used were the Harwell library routine VA05AD, which combines features from the Newton–Raphson, steepest descent and Marquardt methods, and the MINPACK routine LMDIF, which is a modified version of the Levenberg–Marquardt algorithm. Both of these routines have the advantage

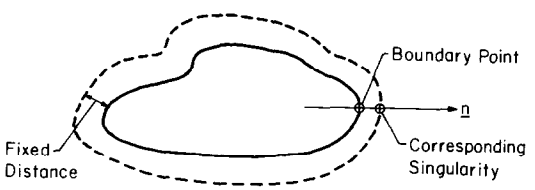

FIG. 1. Initial placement of singularities.

that the user does not have to provide the Jacobian, which is evaluated internally by a finite difference scheme. In the early stages of the experimental work, the efficiency of the two routines was compared using some very simple test problems, and it was found that LMDIF was faster and more economical. Subsequently only LMDIF was used.

4. Some Software Details

In the code used for the numerical solution of the biharmonic equation by the BMFS, the main goal is to minimize the sum of squares

$$F = \sum_{i=1}^{M} \{|B_1 \psi_N(c, d, t, p_i)|^2 + |B_2 \psi_N(c, d, t, p_i)|^2\}. \tag{6}$$

Since the nonlinear least squares routine LMDIF minimizes the sum of squares

$$F = \sum_{i=1}^{K} |f_i|^2, \tag{7}$$

we therefore provide LMDIF with

$$f_i = \alpha(p_i) + \sum_{j=1}^{N} c_j K_1(t_j, p_i) + \sum_{j=1}^{N} d_j K_2(t_j, p_i), \qquad i = 1, 2, \ldots, M \tag{8}$$

and

$$f_i = \beta(p_i) + \sum_{j=1}^{N} c_j \frac{\partial}{\partial n} K_1(t_j, p_i) + \sum_{j=1}^{N} d_j \frac{\partial}{\partial n} K_2(t_j, p_i) \qquad \text{(case (i))}$$

or

$$f_i = \beta(p_i) + \sum_{j=1}^{N} c_j \nabla^2 K_1(t_j, p_i) \qquad i = M+1, \ldots, 2M \quad \text{(case (ii))}, \tag{9}$$

i.e., $K = 2M$.

Further, the code was written to take advantage of two cases of symmetry. In the case where the problem possesses symmetry about one of the coordinate axes, only half the region is considered, in the sense that boundary points are placed on only half the boundary and singularities are placed in only the half plane containing the part of the region we are examining. When the problem is symmetric about both coordinate axes, only a quarter of the region need be considered. In many cases, this feature of the code reduces the size of the minimization problem substantially with a concomitant reduction in computing time.

The minimization routine LMDIF produces the residuals f_i, $i = 1, 2, \ldots, 2M$, and the sum of squares,

$$\text{SSR} = \sum_{i=1}^{2M} |f_i|^2. \tag{10}$$

The computational effort is measured in terms of the number of function evaluations, i.e., the number of times the vector $f = [f_1,...,f_{2M}]$ has to be evaluated. The subroutine LMDIF terminates when convergence to a user-specified tolerance is achieved or when a user-specified limit on the number of function evaluations is reached.

Details concerning the evaluation of the expressions (9) for the various cases of symmetry are given in the Appendix.

5. Some Simple Test Problems

To test the code, the BMFS was used for the solution of some simple problems, whose solutions are known. The numerical results are presented in Table I, where the following notation is used:

EX	the number of the example;
INIT	the boundary points to which the initial singularities correspond, the boundary points being numbered consecutively in a counter-clockwise manner from the positive x-axis;
N	the number of singularities;
M	the number of boundary points;
FEV	the number of function evaluations;
$\|e\|_{\max}$	the maximum error in ψ, ψ' ($\equiv \partial\psi/\partial n$) or $\nabla^2\psi$, as appropriate, at the boundary points p_i, $i = 1,..., M$;
t_1, t_2	the coordinates of the final locations of the singularities;
c, d	the coefficients of K_1 and K_2 in (2).

Example i. $\nabla^4\psi = 0$ on the unit circle with $\psi = x$, and ψ and $\partial\psi/\partial n$ given on the boundary. The problem's symmetry about the x-axis is exploited.

Two singularities were used ($N = 2$) and 31 points placed uniformly on the boundary ($M = 31$). Table I (EX$(i)_\alpha$) shows the results obtained for the absolute values of the maximum errors in ψ and $\partial\psi/\partial n$ on the boundary, the final positions of the singularities and the values of the coefficients c_j and d_j after 300 function evaluations. The accuracy of the method is extremely good. It is interesting to note that the anti-symmetry of the problem about the y-axis is maintained in the final positions of the singularities and the values of the coefficients. Further, we observe that, as the solution is harmonic ($\nabla^2\psi = 0$), the coefficients of the biharmonic fundamental solutions (c_j's) are suppressed.

The same characteristics appear with four ($N = 4$) instead of two singularities ($N = 2$), the difference being that convergence is considerably slower, (Table I, EX$(i)_\beta$).

In both cases the interior of the circle was divided using a uniform grid. The errors for ψ at the grid points were found to be less than the maximum error for ψ on the boundary.

TABLE I

Test Problems (Results)

EX	INIT	N	M	FEV	$\lvert e\rvert_{\max}$ ψ	$\lvert e\rvert_{\max}$ ψ' or $\nabla^2\psi$	t_1	t_2	c	d
i_α	7	2	31	302	0.8824	0.9955	$0.1595\cdot 10^{3}$	$0.9206\cdot 10^{2}$	$0.2630\cdot 10^{-5}$	$-0.2658\cdot 10^{2}$
	25				10^{-8}	10^{-9}	$-0.1595\cdot 10^{3}$	$0.9206\cdot 10^{2}$	$0.2630\cdot 10^{-5}$	$0.2658\cdot 10^{2}$
i_β	5	4	31	309	0.1482	0.3355	$0.3458\cdot 10$	$0.1062\cdot 10$	$-0.1400\cdot 10^{-2}$	-0.3160
	10				10^{-4}	10^{-4}	$0.2362\cdot 10$	$0.3063\cdot 10$	$0.2542\cdot 10^{-2}$	-0.2609
	22						$-0.2244\cdot 10$	$0.3065\cdot 10$	$-0.2483\cdot 10^{-2}$	0.2300
	27						$-0.3571\cdot 10$	$0.1148\cdot 10$	$0.1466\cdot 10^{-2}$	0.3528
ii	10	1	20	302	0.1507	0.9880	$0.1633\cdot 10^{-2}$	$0.6767\cdot 10$	$0.1952\cdot 10^{2}$	$-0.3572\cdot 10^{2}$
					10^{-3}	10^{-4}				
iii	10	2	40	302	0.8781	0.9554	$0.1035\cdot 10^{3}$	$0.5976\cdot 10^{2}$	$0.3225\cdot 10^{-4}$	$-0.1725\cdot 10^{2}$
	31				10^{-8}	10^{-9}	$-0.1035\cdot 10^{3}$	$0.5976\cdot 10^{2}$	$-0.3226\cdot 10^{-4}$	$0.1725\cdot 10^{2}$
iv	7	2	20	303	0.3638	0.5098	$0.2269\cdot 10$	0.8778	$0.1024\cdot 10$	-0.5525
	14				10^{-3}	10^{-3}	0.5167	0.8382	$0.7310\cdot 10^{-1}$	$0.7665\cdot 10^{-3}$
v	7	2	31	302	0.8776	0.8256	$0.1493\cdot 10^{3}$	$0.8627\cdot 10^{2}$	$-0.3558\cdot 10^{-4}$	$-0.2490\cdot 10^{2}$
	25				10^{-8}	10^{-9}	$-0.1493\cdot 10^{3}$	$0.8627\cdot 10^{2}$	$0.3558\cdot 10^{-4}$	$0.2490\cdot 10^{2}$
vi	7	3	31	1300	0.2711	0.7022	$0.4344\cdot 10$	$0.1465\cdot 10$	$0.1529\cdot 10$	$-0.2173\cdot 10$
	16				10^{-4}	10^{-4}	$0.5650\cdot 10^{-15}$	$0.3987\cdot 10$	$0.1483\cdot 10$	$0.1066\cdot 10$
	25						$-0.4344\cdot 10$	$0.1465\cdot 10$	$0.1524\cdot 10$	$-0.2173\cdot 10$
vii	10	2	28	202	0.1141	0.6205	$0.2466\cdot 10$	$0.1022\cdot 10$	$0.1234\cdot 10$	-0.6530
	19				10^{-4}	10^{-5}	$0.1022\cdot 10$	$0.2466\cdot 10$	$0.1234\cdot 10$	-0.6530

EXAMPLE ii. $\nabla^4\psi = 0$ in the unit circle with $\psi = x^2$, and ψ and $\partial\psi/\partial n$ given on the boundary. The symmetry of the problem about both the x- and y-axes is exploited.

For this problem, one singularity was used with 20 boundary points ($N = 1$, $M = 20$). After 300 function evaluations, the maximum errors on the boundary for ψ and $\partial\psi/\partial n$ are of order 10^{-3} and 10^{-4}, respectively. Examination of the error at interior points showed that the maximum error in ψ appeared on the boundary.

EXAMPLE iii. $\nabla^4\psi = 0$ in the unit square with $\psi = x$, and ψ and $\partial\psi/\partial n$ given on the boundary. The problem's symmetry about the x-axis is exploited.

Two singularities were used along with forty boundary points ($N = 2$, $M = 40$) and accuracy of order 10^{-8} is obtained. Again, the anti-symmetry of the problem is preserved, the coefficients of the biharmonic fundamental solutions are suppressed, and examination of the error for ψ at interior points shows that the maximum error for ψ appears on the boundary. Further, in this case, although the region contains corners, the error is uniform around the boundary (for both ψ and $\partial\psi/\partial n$) and the maximum error does not appear at the corners as experienced using a BEM for the same problem [21].

EXAMPLE iv. $\nabla^4\psi = 0$ in the unit square with $\psi = x^2$, given ψ and $\partial\psi/\partial n$ on the boundary. Symmetry about both coordinate axes is exploited.

After 300 function evaluations with two singularities and 20 boundary points ($N = 2$, $M = 20$), accuracy of order 10^{-3} was obtained, and examination of the error for ψ at interior points indicated that it reaches its maximum on the boundary.

EXAMPLE v. $\nabla^4\psi = 0$ in an ellipse with semi-axes $a = 1.0$ and $b = 0.8$ with $\psi = x$, and ψ and $\partial\psi/\partial n$ given on the boundary. Symmetry about the x-axis was exploited and the error for ψ on the boundary was of order 10^{-8} for $N = 2$, $M = 31$ after 300 function evaluations.

EXAMPLE vi. $\nabla^4\psi = 0$ in an ellipse with semi-axes $a = 1.0$ and $b = 0.8$, with $\psi = x^2$, and ψ and $\partial\psi/\partial n$ given on the boundary. In this example, symmetry was exploited only about the x-axis (although the problem has symmetry about both axes). This was done to check that the symmetry about the y-axis is maintained and to examine the effect on the efficiency of the method of not exploiting the symmetry of the problem to the full.

With $N = 3$ and $M = 31$, as many as 1300 function evaluations were required to obtain accuracy of order 10^{-4}. The symmetry is, however, maintained and one of the singularities is eventually located on the y axis.

EXAMPLE vii. $\nabla^4\psi = 0$ in the unit square with $\psi = x^2 + y^2$, given ψ and $\nabla^2\psi$ on the boundary. Symmetry about both axes is exploited. Two singularities with 28 boundary points ($N = 2$, $M = 28$) produce accurate results (of order 10^{-4} and 10^{-5}) after only 200 function evaluations. Symmetry about the line $y = x$ is also preserved (Table I).

The application of the BMFS to these simple test problems provided us with some useful information about the method and the way it is applied. First, the method proved very accurate and convergence was rapid for a small number of singularities and boundary points. We found that, in general, increasing the number of singularities slowed down the convergence of the minimization process. For such simple problems, however, a small number of singularities describes the problem sufficiently well, and therefore convergence is fast on the whole. The second important conclusion is that unlike BEMs and other boundary methods, the accuracy of the BMFS is not affected by the presence of corners (see discussion in Sect. 9). The error in both ψ and $\partial\psi/\partial n$ (or $\nabla^2\psi$) was uniform around the boundary, whether the latter included corners or not. Finally, in all of the examples, the error for ψ was evaluated at numerous interior points and it was observed that the error for ψ reached its maximum on the boundary. Unfortunately, this cannot be verified theoretically as is the case for harmonic problems [30] because no maximum principle exists for biharmonic problems, as it does for harmonic problems.

TABLE II

CPU Times

N	M	FEV	CPU time (min.)
1	20	302	0.049
2	20	303	0.07
2	31	302	0.07
2	40	300	0.084
4	31	309	0.11
4	31	3009	0.92
9	60	3010	3.6

An obvious disadvantage of the BMFS over other boundary methods is its computational cost [20]. Except for the set-up cost and accuracy factors, an important compensating factor is the fact that accuracy is not affected by the shape of the region under consideration. This is due to the freedom the singularities are given, which in a sense absorbs the effect that, for example, a corner could have on the accuracy of the method.

The CPU times in minutes required for various problems are listed in Table II. The computations were performed in double precision on an IBM 3081 computer at the University of Kentucky.

6. An Improved BMFS

In applications of the MFS to second-order elliptic problems, it has been observed [31] that using a block of singularities by block of singularities technique could be advantageous. This technique involves working with a fixed number of singularities $\hat{N}_1$ (say) for a certain number of function evaluations, then leaving those singularities fixed and working with another set of $\hat{N}_2$ singularities for a further number of function evaluations, and so on. This technique does not increase the size of the nonlinear problem to be solved at any time, while increasing the number of singularities.

Attempts to use the same technique with the BMFS showed little or no effect on the efficiency of the method. Instead, another idea, developed by MacDonell [28], proved very successful. This idea comes from the fact that, when using the method of fundamental solutions, it is difficult to decide a priori how many singularities to use to describe the problem satisfactorily. MacDonell [28] in the solution of the three-dimensional modified Helmholtz equation, introduced the idea of starting with a certain number of singularities, N say, and after a certain number of function evaluations increase the number of singularities to N_{new}, by adding extra singularities and iterating further until the required accuracy is reached.

The efficiency of the above scheme for the BMFS is demonstrated in the solution of a simple problem, previously considered by Bogomolny [5], namely:

Solve $\nabla^4\psi = 0$ on the unit circle, given ψ and $\partial\psi/\partial n$ on the boundary, when the problem has the solution $\psi = x^2 + y^2 + x + y$.

This problem has symmetry about the line $y = x$, which can be exploited by rotating the axes by $\pi/4$, in which case:

$$\begin{aligned} x^* &= x\cos(\pi/4) + y\sin(\pi/4), \\ y^* &= -x\sin(\pi/4) + y\cos(\pi/4), \end{aligned} \tag{11}$$

and the problem becomes (dropping the *'s):

$\nabla^4\psi = 0$ in the unit circle, given ψ and $\partial\psi/\partial n$ on the boundary, with solution $\psi = x^2 + y^2 + x\sqrt{2}$.

Taking advantage of the symmetry of the problem about the x axis, the BMFS was applied with $N = 4$ and $M = 31$. After 500 function evaluations, 10^{-3} accuracy was achieved. (See Table III, EX(a)). Next, the BMFS was started with $N = 2$ and $M = 31$. After 200 function evaluations, the number of singularities was increased to four ($N_{\text{new}} = 4$) by adding singularities at locations indicated by INIT_{new}, while the number of boundary points was increased to 48 ($M_{\text{new}} = 48$) (Table III, EX(d)).

TABLE III

Improved BMFS

EX	INIT	N	M	FEV	$\lvert e\rvert_{\max}$ ψ	$\lvert e\rvert_{\max}$ ψ'	t_1	t_2	c	d
(a)	5	4	31	500	0.1399	0.5034	0.3068 · 10	0.1055 · 10	0.9338	−0.1162 · 10
	10				10^{-3}	10^{-3}	0.1797 · 10	0.2576 · 10	0.5862	−0.7481
	20						−0.4259	0.4700 · 10	0.3670 · 10	−0.2006 · 10
	25						−0.4734	0.2525 · 10	0.4726 · 10	−0.2279 · 10
(b)	10	2	31	1000	0.4107	0.1348	$0.2313 \cdot 10^2$	$0.2268 \cdot 10^2$	$0.1401 \cdot 10^3$	$-0.1401 \cdot 10^3$
	20				10^{-3}	10^{-2}	$-0.2335 \cdot 10^2$	$0.2382 \cdot 10^2$	$0.1559 \cdot 10^3$	$-0.1385 \cdot 10^3$
(c)	5	4	31	1000	0.5408	0.2539	0.3446 · 10	0.1211 · 10	0.1177 · 10	−0.1344 · 10
	10				10^{-4}	10^{-3}	0.1992 · 10	0.3069 · 10	0.9464 · 10	−0.1064 · 10
	20						−0.7543	0.4934 · 10	0.3625 · 10	−0.2126 · 10
	25						−0.5021 · 10	0.2600 · 10	0.4928 · 10	−0.2363 · 10
(d)	10	2	31	200	0.7116	0.8674	$0.1217 \cdot 10^2$	$0.1173 \cdot 10^2$	$0.4204 \cdot 10^2$	$-0.4166 \cdot 10^2$
	20				10^{-2}	10^{-2}	$-0.1152 \cdot 10^2$	$0.1198 \cdot 10^2$	$0.4153 \cdot 10^2$	$-0.3282 \cdot 10^2$
	INIT_{new}	N_{new}	M_{new}	FEV	$\lvert e\rvert_{\max}$ ψ	$\lvert e\rvert_{\max}$ ψ'	t_1	t_2	c	d
(d)	10	4	48	200	0.5498	0.8134	$0.2708 \cdot 10^2$	$0.2659 \cdot 10^2$	$0.1913 \cdot 10^3$	$-0.1911 \cdot 10^3$
(contd)	38				10^{-5}	10^{-5}	$-0.2662 \cdot 10^2$	$0.2712 \cdot 10^2$	$0.2038 \cdot 10^3$	$-0.1836 \cdot 10^3$
							0.2105 · 10	0.2037 · 10	$-0.2838 \cdot 10^{-1}$	$0.2935 \cdot 10^{-2}$
							−0.2394 · 10	0.2465 · 10	$-0.5356 \cdot 10^{-1}$	$0.9150 \cdot 10^{-2}$

The process was then continued, with the initial singularities starting from their locations after the first 200 function evaluations and the new ones placed at certain initial positions chosen by the user. With only 200 extra function evaluations, accuracy of 10^{-5} was obtained (Table III, EX(d)(contol)). The error was also evaluated at points on a uniform grid in the interior and it was observed that the maximum error occurred on the boundary.

Table III also shows the results for 1000 function evaluations with $N=4$ and $M=31$ (EX(c)), and 1000 function evaluations for $N=2$, $M=31$ (EX(b)). It is noteworthy that the accuracy reached by the improved version of the BMFS after a total of only 400 function evaluations cannot be achieved by the ordinary version of the BMFS, even after a considerable number of function evaluations.

In principle, we could add more singularities and increase the number of boundary points after the second stage of the improved scheme. However, this can become counterproductive in that the size of the nonlinear minimization problem would increase considerably, thus requiring a large amount of computing time. For the problem we are examining, adding just one extra set of singularities is both cheap and efficient. It should be mentioned at this point that the initial positions of the new singularities are chosen in such a way as to be spread uniformly around the boundary. This is applied in general, unless there is good reason to place them near a particular point (see Sect. 8).

The improved version of the BMFS was next applied to some more difficult problems from the theory of elasticity (Sect. 7).

7. Application of the BMFS to Thin Plate Bending Problems

i. *The General Problem*

The transverse deflection of a thin plate under a uniform load K per unit area satisfies [38],

$$\nabla^4 w = K/D, \tag{12}$$

where D is the bending rigidity. When the plate is clamped, the conditions on the boundary are

$$\begin{aligned} w &= 0, \\ \frac{\partial w}{\partial n} &= 0, \end{aligned} \tag{13}$$

whereas when the plate is simply supported, they are

$$\begin{aligned} w &= 0, \\ \nabla^2 w &= 0. \end{aligned} \tag{14}$$

In the following way, the above problems can be easily transformed to biharmonic problems of the forms already encountered (cf. [17]).

Let

$$\psi_1 = \frac{(x^2+y^2)^2}{64} = \frac{r^4}{64}. \tag{15}$$

Then if we write

$$w = (\psi + \psi_1) \cdot K/D, \tag{16}$$

it follows that

$$\nabla^4 \psi = 0$$

subject to either

$$\begin{aligned} \psi &= \frac{-r^4}{64}, \\ \frac{\partial \psi}{\partial n} &= -\frac{\partial}{\partial n}\left(\frac{r^4}{64}\right) \end{aligned} \tag{17}$$

in the case of a clamped plate, or

$$\begin{aligned} \psi &= \frac{-r^4}{64}, \\ \nabla^2 \psi &= -\nabla^2\left(\frac{r^4}{64}\right) = \frac{-r^2}{4} \end{aligned} \tag{18}$$

in the case of a simply supported plate. The BMFS can now be applied to either of these problems. Once the minimization procedure is completed and the variables are determined, ψ_N can be evaluated at any point in the region. Then, the deflection w can be determined at these points by using

$$w = (\psi_N + \psi_1) \cdot \frac{K}{D}, \qquad \text{i.e.,} \quad w = \left(\psi_N + \frac{r^4}{64}\right) \cdot \frac{K}{D}. \tag{19}$$

ii. *Clamped Elliptic Plate*

This problem was previously considered by Murashima, Nonaka, and Nieda [32] using a MFS-type method in which the solution is of the form (2), but the locations of the singularities are fixed and the coefficients c_j and d_j, $j = 1,..., N$, are determined by collocating the boundary conditions at $2N$ distinct points and solving the resulting linear system by Gauss elimination. The semi-major axis of the ellipse was taken to be $a = 1.0$ and the semi-minor axis to be $b = 0.8333$.

The problem for ψ has symmetry about both the x- and y-axes, and if this symmetry is exploited in the BMFS, only a quarter of the plate has to be considered.

The BMFS was applied to the problem for various numbers of singularities (and boundary points), and some of the results are displayed in Table IV. The improved version of the BMFS was also employed and, as shown in Table IV, there is substantial improvement in both the accuracy of the results and the convergence of the method.

iii. *Simply Supported Square Plate*

A different geometry was next examined, in the sense that the region (the unit square) contains corners. Further, the plate is assumed to be simply supported instead of clamped. The problem has symmetry about both coordinate axes and, exploiting this fact, the BMFS need be applied to only a quarter of the region.

This problem was also considered by Murashima *et al.* [32]. However, they

TABLE VI

Simply Supported Elliptic Plate with Hole

INIT	$\tilde{N}_1$	$\tilde{N}_2$	M_1	M_2	FEV	$\lvert e\rvert_{\max}$ ψ	$\lvert e\rvert_{\max}$ $\nabla^2\psi$	t_1	t_2	c	d
4	2	2	12	12	200	0.4432	0.6422	$0.1758 \cdot 10$	0.6692	$0.2136 \cdot 10^{-1}$	$0.2365 \cdot 10^{-1}$
8						10^{-3}	10^{-3}	0.8067	$0.1728 \cdot 10$	$-0.6665 \cdot 10^{-1}$	$-0.6271 \cdot 10^{-2}$
16								$0.6772 \cdot 10^{-1}$	$0.2502 \cdot 10^{-1}$	$-0.3169 \cdot 10^{-2}$	$0.4624 \cdot 10^{-3}$
20								$0.3873 \cdot 10^{-1}$	$0.8705 \cdot 10^{-1}$	$-0.1545 \cdot 10^{-2}$	$0.9490 \cdot 10^{-4}$
4	2	2	12	12	500	0.3158	0.2671	$0.2297 \cdot 10$	0.9971	$0.9125 \cdot 10^{-1}$	$0.6728 \cdot 10^{-1}$
8						10^{-3}	10^{-3}	$0.1149 \cdot 10$	$0.2185 \cdot 10$	-0.1464	$-0.4063 \cdot 10^{-1}$
16								$0.7013 \cdot 10^{-1}$	$0.3125 \cdot 10^{-1}$	$-0.3256 \cdot 10^{-2}$	$0.4650 \cdot 10^{-3}$
20								$0.3287 \cdot 10^{-1}$	$0.8669 \cdot 10^{-1}$	$-0.1477 \cdot 10^{-2}$	$0.9341 \cdot 10^{-4}$
3	3	1	12	12	500	0.7952	0.7036	$0.2145 \cdot 10$	0.5516	$0.4464 \cdot 10^{-1}$	$0.2907 \cdot 10^{-1}$
6						10^{-4}	10^{-5}	$0.1556 \cdot 10$	$0.1586 \cdot 10$	$-0.3326 \cdot 10^{-1}$	$0.5844 \cdot 10^{-2}$
10								0.5864	$0.1993 \cdot 10$	$0.5622 \cdot 10^{-1}$	$-0.1444 \cdot 10^{-1}$
18								$0.3032 \cdot 10^{-1}$	$0.1223 \cdot 10^{-1}$	$-0.4313 \cdot 10^{-2}$	$0.5348 \cdot 10^{-3}$
5	3	1	24	24	500	0.7975	0.7571	$0.2178 \cdot 10$	0.5599	$0.4841 \cdot 10^{-1}$	$0.3104 \cdot 10^{-1}$
12						10^{-4}	10^{-5}	$0.1587 \cdot 10$	$0.1634 \cdot 10$	$-0.3505 \cdot 10^{-1}$	$0.6353 \cdot 10^{-2}$
19								0.6034	$0.2038 \cdot 10$	$-0.5932 \cdot 10^{-1}$	$-0.1620 \cdot 10^{-1}$
36								$0.3031 \cdot 10^{-1}$	$0.1223 \cdot 10^{-1}$	$-0.4313 \cdot 10^{-2}$	$0.5348 \cdot 10^{-3}$
5	3	2	24	24	500	0.1578	0.2463	$0.1860 \cdot 10$	0.4791	$0.2182 \cdot 10^{-1}$	$0.1740 \cdot 10^{-1}$
12						10^{-4}	10^{-4}	$0.1380 \cdot 10$	$0.1359 \cdot 10$	$-0.2605 \cdot 10^{-1}$	$0.5384 \cdot 10^{-2}$
19								0.4912	$0.1712 \cdot 10$	$-0.3893 \cdot 10^{-1}$	$-0.5432 \cdot 10^{-2}$
32								$0.8436 \cdot 10^{-1}$	$0.2758 \cdot 10^{-1}$	$-0.1677 \cdot 10^{-2}$	$0.2864 \cdot 10^{-3}$
40								$0.3340 \cdot 10^{-1}$	$0.5792 \cdot 10^{-1}$	$-0.2993 \cdot 10^{-3}$	$0.2668 \cdot 10^{-3}$
4	3	2	16	16	500	0.2275	0.4719	$0.1777 \cdot 10$	0.4406	$0.1693 \cdot 10^{-1}$	$0.1519 \cdot 10^{-1}$
8						10^{-4}	10^{-4}	$0.1305 \cdot 10$	$0.1229 \cdot 10$	$-0.1618 \cdot 10^{-1}$	$0.5760 \cdot 10^{-2}$
12								0.5135	$0.1718 \cdot 10$	$-0.4260 \cdot 10^{-1}$	$-0.5129 \cdot 10^{-2}$
21								0.1082	$0.2867 \cdot 10^{-1}$	$-0.4352 \cdot 10^{-3}$	$0.1195 \cdot 10^{-3}$
27								$0.3579 \cdot 10^{-1}$	$0.3844 \cdot 10^{-1}$	$-0.4091 \cdot 10^{-2}$	$0.4254 \cdot 10^{-3}$

8. A Fluid Flow Problem

i. *History*

The driven cavity problem describes steady viscous flow in a square cavity with a sliding wall (Fig. 2). The streamfunction ψ satisfies:

$$\nabla^4\psi = 0 \qquad \text{in } \Omega \tag{20}$$

Subject to

$$\psi = 0, \qquad \frac{\partial\psi}{\partial n} = 0 \qquad \text{on} \quad DABC, \tag{21}$$

$$\psi = 0, \qquad \frac{\partial\psi}{\partial n} = -1 \quad \text{on} \quad CD. \tag{22}$$

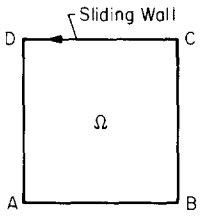

FIG. 2. Driven cavity problem.

This problem has received much attention in the past. Boundary element methods were used by Kelmanson [22] and Ingber and Mitra [15], and an MFS-type method with fixed singularities by Burgess and Mahajerin [7].

The main feature of the problem is the presence of boundary singularities at the corners C and D, where the vorticity, $\nabla^2\psi$, and its normal derivative $\partial\nabla^2\psi/\partial n$ become unbounded. This, in conjunction with the presence of the other two corners in the region, can produce poor results in the whole region when a direct BEM is used with piecewise constant approximations [22]. This is apparently avoided when a subtraction of the singularity technique is used. When an indirect BEM is used, more satisfactory results are obtained by Ingber and Mitra [15] however with higher-order boundary elements (quadratic).

ii. *Application of the* BMFS

The problem has symmetry about the line through the midpoints of the sides AB and CD, and this is exploited when using the BMFS, as only half the region needs to be considered (Fig. 3). Due to the presence of the boundary singularity at D, a relatively large number of singularities (and boundary points) is required to describe the problem. Further, a denser grid was taken near the singularity by choosing boundary points of the form

$$d_j = 0.5 \cdot \left(\frac{M_1 - j}{M_1}\right)^{\alpha} \tag{23}$$

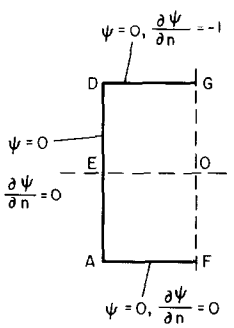

FIG. 3. Symmetry of the driven cavity problem.

where M_1 describes the number of boundary points on either of the sides adjacent to the singularity (GD, DE), d_j describes the distance of the jth-boundary point from D (on both GD and DE, counting j from D). When $\alpha = 1$ a uniform distribution of points is obtained and values of $\alpha > 1$ refine the distribution in the neighbourhood of the boundary singularity. The value $\alpha = 2$ was used, after some experimentation with various values of α.

Also, experiments showed that the BMFS algorithm places several singularities in the neighbourhood of D (Fig. 4). This is a direct result of the presence of the boundary singularity there, as the BMFS approximation is only valid if the auxiliary boundary, formed by the singularities, approaches the boundary of the region under consideration at the singular point [11, 33].

iii. *Three Approaches—Numerical Results*

Three versions of the BMFS were used to solve this problem. Approximations at interior points of the region $0 \leqslant x \leqslant 0.5$, $0 \leqslant y \leqslant 1.0$, obtained using these methods and by Kelmanson [22] using a BEM incorporating a subtraction of singularity technique with 200 boundary segments of equal length, are presented in Table 8 in the format described in Table VII.

First, the ordinary version of the BMFS was applied and it was found that the convergence of the method was very slow. This is a result of both the presence of the boundary singularity and the magnitude of the nonlinear minimization problem ($N = 10$, $M = 80$, say). As many as 5000 function evaluations were necessary to obtain accuracy of order 10^{-3} (Table VIII). The second approach was based on a block-by-block technique. In Section 6 it was mentioned that such techniques were applied when solving simple test problems using the BMFS and little improvement was achieved. For this problem however, because of the magnitude of the minimization problem and the ability of the block-by-block technique to deal with separate sets of singularities, it was hoped that some advantages would be gained by this. This was partially true, as is shown in Table VIII. The third approach was the improved version of the BMFS. This process was started with N uniformly dis-

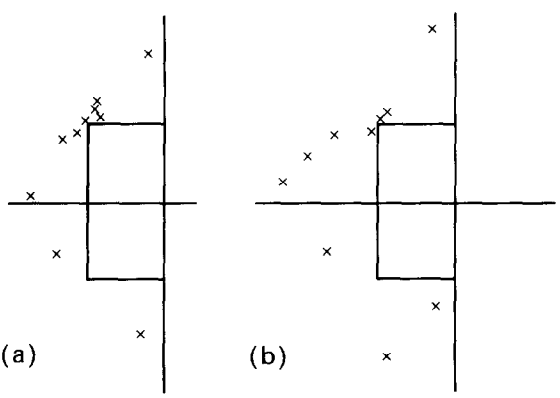

FIG. 4. Observed typical behavior of singularities. (a) $N = 10$, $M = 80$, (b) $N = 10$, $M = 60$.

tributed singularities and, after a certain number of function evaluations, a few more singuarities were added in the neighbourhood of the boundary singularity at D and the process was continued. The results at interior points were tabulated and were found to be in good agreement with those obtained by Kelmanson [22] with a direct BEM incorporating a subtraction of the singularity technique.

Some of the numerical results obtained are presented in Table VIII. It was observed that, in general, at a boundary point the error in ψ was of order 10^{-3} or 10^{-4} with the exception of points near D where the accuracy was lower due to the presence of the boundary singularity at this point.

On the whole, the results for this problem were satisfactory. However, a drawback was the large computing cost, as many function evaluations had to be performed to achieve accuracy of order 10^{-3}. This is due to the presence of the boundary singularity and the magnitude of the nonlinear minimization problem. On the other hand, the results at interior points were very satisfactory and although little was done to describe the singularity, this did not affect interior values substantially. Figure 5 is a contour plot of the streamlines in the region $0 \leqslant x \leqslant 0.5$, $0 \leqslant y \leqslant 1.0$ using mesh 4 of Table VIII. This describes accurately the flow (cf. [22]).

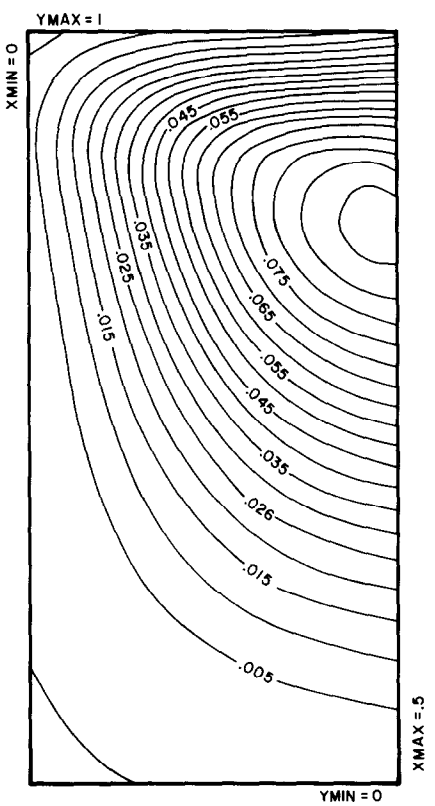

FIG. 5. Streamfunction contour.

9. Comments and Conclusions

The BMFS in its various forms has proved to be a powerful numerical method for the solution of biharmonic problems. Like BEMs, it requires that only the boundary of the region be discretized, which is extremely useful for problems where only the solution on the boundary is required. Further, the data preparation is very easy and cheap. In the BMFS, relatively few boundary points and singularities are required to produce accurate numerical results. This is in contrast with other boundary methods, for which a denser discretization is required and, in general, more terms have to be used in the approximation function to obtain comparable accuracy. Unlike BEMs, the BMFS does not involve integrations, which can, in some cases, prove tedious and expensive, especially when higher-order elements are used. Probably the most important feature of the BMFS is the fact that the freedom of movement that the singularities are allowed (although we pay for it in computing time) produces a uniform distribution of the error on the boundary regardless of the shape of the latter. In particular, corners in the region do not provide a particular source of inaccuracy. This is a feature which is not, on the whole, shared by BEMs where it has been either mentioned in the literature [12, 16, 17, 29, 34] or observed [22] that corners are sources of large errors. The same problem seems to appear in the application of the MFS method of [32] to biharmonic problems containing corners.

A criticism of the BMFS could be its computational cost arising from the use of the nonlinear least squares minimization routine. However, no attempt has been made to exploit the structure of the functional to be minimized, in which the coefficients of the fundamental solutions (c_j, d_j) are linear and only the coordinates of the singularities appear nonlinearly. Moreover, for convenience, we have chosen to use the subroutine LMDIF which calculates an approximation to the Jacobian. The

TABLE VII

Description of Table VIII

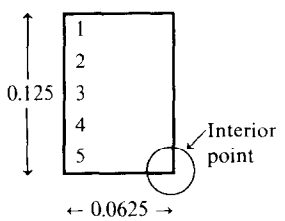

(1) BMFS, $M = 80$, $N = 10$, FEV = 5000.
(2) Block-by-block BMFS, $M = 96$, $\hat{N}_1 = 10$, $\hat{N}_2 = 10$, FEV = 2000.
(3) Improved BMFS, $M = 96$, $N = 9$, $M_{\text{new}} = 132$, $N_{\text{new}} = 12$, FEV = 2000.
(4) Improved BMFS, $M = 96$, $N = 9$, $M_{\text{new}} = 132$, $N_{\text{new}} = 12$, FEV = 3000.
(5) BEM incorporating subtraction of singularity technique [22] (200 boundary segments of equal length).

TABLE VIII

Interior BMFS Values for ψ

0.0135	0.0372	0.0548	0.0665	0.0742	0.0791	0.0818	0.0827
0.0167	0.0350	0.0514	0.0648	0.0749	0.0821	0.0863	0.0877
0.0186	0.0390	0.0558	0.0673	0.0747	0.0792	0.0816	0.0823
0.0150	0.0378	0.0556	0.0674	0.0747	0.0788	0.0807	0.0815
0.0148	0.0378	0.0553	0.0669	0.0745	0.0791	0.0817	0.0825
0.0086	0.0276	0.0487	0.0674	0.0819	0.0920	0.0980	0.0999
0.0066	0.0257	0.0472	0.0667	0.0825	0.0939	0.1007	0.1030
0.0056	0.0258	0.0477	0.0667	0.0814	0.0916	0.0975	0.0994
0.0068	0.0264	0.0480	0.0670	0.0815	0.0915	0.0972	0.0991
0.0086	0.0277	0.0488	0.0675	0.0820	0.0920	0.0979	0.0998
0.0061	0.0187	0.0348	0.0510	0.0650	0.0756	0.0822	0.0844
0.0050	0.0178	0.0343	0.0510	0.0657	0.0768	0.0838	0.0862
0.0050	0.0176	0.0338	0.0502	0.0643	0.0750	0.0816	0.0838
0.0051	0.0178	0.0341	0.0504	0.0645	0.0751	0.0816	0.0837
0.0053	0.0182	0.0345	0.0509	0.0650	0.0756	0.0821	0.0843
0.0030	0.0110	0.0218	0.0333	0.0438	0.0520	0.0573.	0.0590
0.0037	0.0116	0.0223	0.0338	0.0445	0.0529	0.0583	0.0601
0.0032	0.0111	0.0217	0.0330	0.0434	0.0516	0.0568	0.0586
0.0028	0.0109	0.0216	0.0331	0.0435	0.0517	0.0569	0.0586
0.0031	0.0111	0.0219	0.0333	0.0438	0.0520	0.0572	0.0590
0.0010	0.0056	0.0119	0.0188	0.0254	0.0307	0.0341	0.0353
0.0018	0.0062	0.0124	0.0193	0.0259	0.0312	0.0347	0.0359
0.0013	0.0058	0.0120	0.0188	0.0252	0.0304	0.0338	0.0350
0.0015	0.0059	0.0121	0.0189	0.0254	0.0306	0.0340	0.0351
0.0016	0.0061	0.0122	0.0190	0.0255	0.0306	0.0340	0.0352
0.0008	0.0025	0.0052	0.0085	0.0118	0.0146	0.0164	0.0171
−0.0002	0.0019	0.0050	0.0085	0.0119	0.0147	0.0165	0.0172
0.0010	0.0027	0.0053	0.0085	0.0117	0.0144	0.0162	0.0168
0.0010	0.0027	0.0054	0.0086	0.0119	0.0146	0.0164	0.0170
0.0007	0.0026	0.0054	0.0087	0.0119	0.0145	0.0162	0.0168
0.0006	0.0005	0.0008	0.0017	0.0029	0.0042	0.0052	0.0055
−0.0004	−0.0001	0.0007	0.0017	0.0029	0.0040	0.0048	0.0050
0.0004	0.0003	0.0008	0.0017	0.0029	0.0040	0.0048	0.0051
0.0000	0.0002	0.0008	0.0018	0.0030	0.0042	0.0050	0.0052
0.0001	0.0006	0.0013	0.0023	0.0032	0.0040	0.0045	0.0047

use of LMDER, also a MINPACK subroutine, might improve the efficiency of the minimization process but would increase significantly the complexity of the code since LMDER requires the user to supply the exact Jacobian. It was observed that in most problems considered, the computational cost was relatively low, expecially when using the improved version of the BMFS.

Finally, it should be emphasized that the BMFS is not restricted to the two kinds of problems described in Section 3. These were considered because they are

representative of the types of problems most commonly encountered. A minor modification of the code would adapt the BMFS to any combination of boundary conditions and even nonlinear boundary conditions.

APPENDIX

The nonlinear minimization routine minimizes

$$\sum_{i=1}^{M}\left\{\left|\alpha(p_i)+\sum_{j=1}^{N} c_j K_1(t_j,p_i)+\sum_{j=1}^{N} d_j K_2(t_j,p_i)\right|^2+\left|\beta(p_i)+\sum_{j=1}^{N} c_j\frac{\partial}{\partial n}K_1(t_j,p_i)\right.\right.$$
$$\left.\left.+\sum_{j=1}^{N} d_j\frac{\partial}{\partial n}K_2(t_j,p_i)\right|^2\right\} \qquad \text{(case (i))} \tag{A1}$$

or

$$\sum_{i=1}^{M}\left\{\left|\alpha(p_i)+\sum_{j=1}^{N} c_j K_1(t_j,p_i)+\sum_{j=1}^{N} d_j K_2(t_j,p_i)\right|^2\right.$$
$$\left.+\left|\beta(p_i)+\sum_{j=1}^{N} c_j\nabla^2 K_1(t_j,p_i)\right|^2\right\} \qquad \text{case (ii))} \tag{A2}$$

To provide the nonlinear least squares routine with the appropriate sum of squares to be minimized, the following quantities must be evaluated (where $t_j=t$ and $p_i=p$):

$$\begin{aligned} F_1 &= K_1(t,p),\\ F_2 &= K_2(t,p),\\ FN_1 &= \frac{\partial}{\partial n}K_1(t,p),\\ FN_2 &= \frac{\partial}{\partial n}K_2(t,p),\\ FL_1 &= \nabla^2 K_1(t,p). \end{aligned} \tag{A3}$$

When the problem has no symmetry, differentiation gives

$$F_1=\left[\frac{\sqrt{(t_1-p_1)^2+(t_2-p_2)^2}}{\rho+\sqrt{t_1^2+t_2^2}}\right]^2\log\left[\frac{\sqrt{(t_1-p_1)^2+(t_2-p_2)^2}}{\rho+\sqrt{t_1^2+t_2^2}}\right]^2, \tag{A4}$$

$$F_2=\log\left[\frac{\sqrt{(t_1-p_1)^2+(t_2-p_2)^2}}{\rho+\sqrt{t_1^2+t_2^2}}\right]^2, \tag{A5}$$

$$FN_1 = \frac{1}{(\rho + \sqrt{t_1^2 + t_2^2})^2}\left[\log\left(\frac{\sqrt{(t_1-p_1)^2+(t_2-p_2)^2}}{\rho+\sqrt{t_1^2+t_2^2}}\right)^2 + 1\right] \times \left[2(p_1-t_1)\frac{\partial p_1}{\partial n} + 2(p_2-t_2)\frac{\partial p_2}{\partial n}\right], \tag{A6}$$

$$FN_2 = \frac{2(p_1-t_1)(\partial p_1/\partial n) + 2(p_2-t_2)(\partial p_2/\partial n)}{(t_1-p_1)^2+(t_2-p_2)^2}, \tag{A7}$$

$$FL_1 = \frac{4}{(\rho+\sqrt{t_1^2+t_2^2})^2}\left[\log\left(\frac{\sqrt{(t_1-p_1)^2+(t_2-p_2)^2}}{\rho+\sqrt{t_1^2+t_2^2}}\right)^2 + 2\right], \tag{A8}$$

where $(\partial p_1/\partial n, \partial p_2/\partial n)$ are the direction cosines of the boundary point p. When the problem has symmetry about the x-axis, terms have to be added twice because, for a contribution from a boundary point (p_1, p_2), there will correspond a boundary point $(p_1, -p_2)$ below the x-axis, and the two have to be added in the sums (A1) and (A2). Thus the terms are modified as follows:

$$F_1 = \left[\frac{\sqrt{(t_1-p_1)^2+(t_2-p_2)^2}}{\rho+\sqrt{t_1^2+t_2^2}}\right]^2 \log\left[\frac{\sqrt{(t_1-p_1)^2+(t_2-p_2)^2}}{\rho+\sqrt{t_1^2+t_2^2}}\right]^2 + \left[\frac{\sqrt{(t_1-p_1)^2+(t_2-p_2)^2+4t_2p_2}}{\rho+\sqrt{t_1^2+t_2^2}}\right]^2 \log\left[\frac{\sqrt{(t_1-p_1)^2+(t_2-p_2)^2+4t_2p_2}}{\rho+\sqrt{t_1^2+t_2^2}}\right]^2 \tag{A9}$$

$$F_2 = \log\left[\frac{\sqrt{(t_1-p_1)^2+(t_2-p_2)^2}\sqrt{(t_1-p_1)^2+(t_2-p_2)^2+4t_2p_2}}{(\rho+\sqrt{t_1^2+t_2^2})^2}\right]^2 \tag{A10}$$

$$FN_1 = \frac{1}{(\rho+\sqrt{t_1^2+t_2^2})^2}\cdot\left\{\left[\log\left(\frac{\sqrt{(t_1-p_1)^2+(t_2-p_2)^2}}{\rho+\sqrt{t_1^2+t_2^2}}\right)^2+1\right]\cdot\left[2(p_1-t_1)\frac{\partial p_1}{\partial n}+2(p_2-t_2)\frac{\partial p_2}{\partial n}\right] + \left[\log\left(\frac{\sqrt{(t_1-p_1)^2+(t_2-p_2)^2+4t_2p_2}}{\rho+\sqrt{t_1^2+t_2^2}}\right)^2+1\right]\cdot\left[2(p_1-t_1)\frac{\partial p_1}{\partial n}+2(p_2+t_2)\frac{\partial p_2}{\partial n}\right]\right\}, \tag{A11}$$

$$FN_2 = \frac{2(p_1-t_1)(\partial p_1/\partial n)+2(p_2-t_2)(\partial p_2/\partial n)}{(t_1-p_1)^2+(t_2-p_2)^2} + \frac{2(p_1-t_1)(\partial p_1/\partial n)+2(p_2+t_2)(\partial p_2/\partial n)}{(t_1-p_1)^2+(t_2-p_2)^2+4t_2p_2}, \tag{A12}$$

$$FL_1 = \frac{4}{(\rho + \sqrt{t_1^2 + t_2^2})^2} \cdot \left\{ \log \left[\frac{\sqrt{(t_1 - p_1)^2 + (t_2 - p_2)^2} \cdot \sqrt{(t_1 - p_1)^2 + (t_2 - p_2)^2 + 4t_2 p_2}}{(\rho + \sqrt{t_1^2 + t_2^2})^2} \right]^2 + 4 \right\}. \tag{A13}$$

When the problem has symmetry about both the x- and the y-axes, contributions from three more points have to be considered for each point (p_1, p_2), namely,

$(-p_1, p_2)$ in the second quadrant,

$(p_1, -p_2)$ in the fourth quadrant,

and

$(-p_1, -p_2)$ in the third quadrant.

This yields the modifications

$$\begin{aligned} F_1 = {} & \left[\frac{\sqrt{(t_1 - p_1)^2 + (t_2 - p_2)^2}}{\rho + \sqrt{t_1^2 + t_2^2}} \right]^2 \log \left[\frac{\sqrt{(t_1 - p_1)^2 + (t_2 - p_2)^2}}{\rho + \sqrt{t_1^2 + t_2^2}} \right]^2 \\ & + \left[\frac{\sqrt{(t_1 - p_1)^2 + (t_2 - p_2)^2 + 4t_2 p_2}}{\rho + \sqrt{t_1^2 + t_2^2}} \right]^2 \log \left[\frac{\sqrt{(t_1 - p_1)^2 + (t_2 - p_2)^2 + 4t_2 p_2}}{\rho + \sqrt{t_1^2 + t_2^2}} \right]^2 \\ & + \left[\frac{\sqrt{(t_1 - p_1)^2 + (t_2 - p_2)^2 + 4t_1 p_1}}{\rho + \sqrt{t_1^2 + t_2^2}} \right]^2 \log \left[\frac{\sqrt{(t_1 - p_1)^2 + (t_2 - p_2)^2 + 4t_1 p_1}}{\rho + \sqrt{t_1^2 + t_2^2}} \right]^2 \\ & + \left[\frac{\sqrt{(t_1 - p_1)^2 + (t_2 - p_2)^2 + 4(t_1 p_1 + t_2 p_2)}}{\rho + \sqrt{t_1^2 + t_2^2}} \right]^2 \\ & \times \log \left[\frac{\sqrt{(t_1 - p_1)^2 + (t_2 - p_2)^2 + 4(t_1 p_1 + t_2 p_2)}}{\rho + \sqrt{t_1^2 + t_2^2}} \right]^2 \end{aligned} \tag{A14}$$

$$\begin{aligned} F_2 = {} & \log \left[\frac{\sqrt{(t_1 - p_1)^2 + (t_2 - p_2)^2}}{\rho + \sqrt{t_1^2 + t_2^2}} \right]^2 \\ & + \log \left[\frac{\sqrt{(t_1 - p_1)^2 + (t_2 - p_2)^2 + 4t_2 p_2}}{\rho + \sqrt{t_1^2 + t_2^2}} \right]^2 \\ & + \log \left[\frac{\sqrt{(t_1 - p_1)^2 + (t_2 - p_2)^2 + 4t_1 p_1}}{\rho + \sqrt{t_1^2 + t_2^2}} \right]^2 \\ & + \log \left[\frac{\sqrt{(t_1 - p_1)^2 + (t_2 - p_2)^2 + 4(t_1 p_1 + t_2 p_2)}}{\rho + \sqrt{t_1^2 + t_2^2}} \right]^2 \end{aligned} \tag{A15}$$

$$FN_1 = \frac{1}{(\rho+\sqrt{t_1^2+t_2^2})^2}\cdot\left\{\left[\log\left(\frac{\sqrt{(t_1-p_1)^2+(t_2-p_2)^2}}{\rho+\sqrt{t_1^2+t_2^2}}\right)^2+1\right]\right.$$
$$\cdot\left[2(p_1-t_1)\frac{\partial p_1}{\partial n}+2(p_2-t_2)\frac{\partial p_2}{\partial n}\right]$$
$$+\left[\log\left(\frac{\sqrt{(t_1-p_1)^2+(t_2-p_2)^2+4t_2p_2}}{\rho+\sqrt{t_1^2+t_2^2}}\right)^2+1\right]$$
$$\cdot\left[2(p_1-t_1)\frac{\partial p_1}{\partial n}+2(p_2+t_2)\frac{\partial p_2}{\partial n}\right]$$
$$+\left[\log\left(\frac{\sqrt{(t_1-p_1)^2+(t_2-p_2)^2+4t_1p_1}}{\rho+\sqrt{t_1^2+t_2^2}}\right)^2+1\right]$$
$$\cdot\left[2(p_1+t_1)\frac{\partial p_1}{\partial n}+2(p_2-t_2)\frac{\partial p_2}{\partial n}\right]$$
$$+\left[\log\frac{\sqrt{(t_1-p_1)^2+(t_2-p_2)^2+4(t_1p_1+t_2p_2)}}{\rho+\sqrt{t_1^2+t_2^2}}\right)^2+1\Bigg]$$
$$\left.\cdot\left[2(p_1+t_1)\frac{\partial p_1}{\partial n}+2(p_2+t_2)\frac{\partial p_2}{\partial n}\right]\right\}, \tag{A16}$$

$$\frac{2(p_1-t_1)(\partial p_1/\partial n)+2(p_2-t_2)(\partial p_2/\partial n)}{(t_1-p_1)^2+(t_2-p_2)^2}$$
$$+\frac{2(p_1-t_1)(\partial p_1/\partial n)+2(p_2+t_2)(\partial p_2/\partial n)}{(t_1-p_1)^2+(t_2-p_2)^2+4t_2p_2}$$
$$+\frac{2(p_1+t_1)(\partial p_1/\partial n)+2(p_2-t_2)(\partial p_2/\partial n)}{(t_1-p_1)^2+(t_2-p_2)^2+4t_1p_1}$$
$$+\frac{2(p_1+t_1)(\partial p_1/\partial n)+2(p_2+t_2)(\partial p_2/\partial n)}{(t_1-p_1)^2+(t_2-p_2)^2+4(t_1p_1+t_2p_2)}, \tag{A17}$$

$$FL_1 = \frac{4}{(\rho+\sqrt{t_1^2+t_2^2})^2}\cdot\left\{\log\left[\frac{\sqrt{(t_1-p_1)^2+(t_2-p_2)^2}}{\rho+\sqrt{t_1^2+t_2^2}}\right]^2\right.$$
$$+\log\left[\frac{\sqrt{(t_1-p_1)^2+(t_2-p_2)^2+4t_2p_2}}{\rho+\sqrt{t_1^2+t_2^2}}\right]^2$$
$$+\log\left[\frac{\sqrt{(t_1-p_1)^2+(t_2-p_2)^2+4t_1p_1}}{\rho+\sqrt{t_1^2+t_2^2}}\right]^2$$
$$\left.+\log\left[\frac{\sqrt{(t_1-p_1)^2+(t_2-p_2)^2+4(t_1p_1+t_2p_2)}}{\rho+\sqrt{t_1^2+t_2^2}}\right]^2+8\right\}. \tag{A18}$$

REFERENCES

1. M. A. ALEKSIDZE, *Differential Equations* **2**, 515 (1966).
2. P. K. BANERJEE AND R. BUTTERFIELD, *Boundary Element Methods in Engineering Science* (McGraw–Hill, U.K., 1981).
3. G. BÉZINE, *Mech. Res. Comm.* **5**, 197 (1978).
4. J. R. BLACK, M. M. DENN, AND G. C. HSIAO, in *Theoretical Rheology*, edited by J. F. Hutton, *et al.* (Halsted, New York, 1975), p. 3.
5. A. BOGOMOLNY, *SIAM J. Numer. Anal.* **22**, 644 (1985).
6. G. BURGESS AND E. MAHAJERIN, *Comput. & Structures* **19**, 697 (1984).
7. G. BURGESS AND E. MAHAJERIN, *Comput. Fluids* **12**, 311 (1984).
8. C. J. COLEMAN, *Quart. J. Mech. Appl. Math.* **34**, 453 (1981).
9. G. DEMEY, *Comput. & Structures* **8**, 113 (1978).
10. G. FAIRWEATHER, F. J. RIZZO, D. J. SHIPPY, AND Y. S. WU, *J. Comput. Phys.* **31**, 96 (1979).
11. G. FAIRWEATHER AND R. L. JOHNSTON, in *Treatment of Integral Equations by Numerical Methods*, edited by C. T. H. Baker and G. F. Miller (Academic Press, London, 1982), p. 349.
12. G. GOSPODINOV AND D. LJUTSKANOV, *Appl. Math. Modelling* **6**, 237 (1982).
13. U. HEISE, *Comput. & Structures* **8**, 199 (1978).
14. S. HO-TAI, R. L. JOHNSTON, AND R. MATHON, Tech. Report 136/79, Department of Computer Science, University of Toronto, Canada, 1979.
15. M. S. INGBER AND A. K. MITRA, *Int. J. Numer. Methods Eng.* **23**, 2121 (1985).
16. M. A. JASWON, M. MAITI AND G. T. SYMM, *Int. J. Solids and Structures* **3**, 309 (1967).
17. M. A. JASWON AND M. MAITI, *J. Eng. Math.* **2**, 83 (1968).
18. M. A. JASWON AND G. T. SYMM, *Integral Equation Methods in Potential Theory and Elastostatics* (Academic Press, New York, 1977).
19. R. L. JOHNSTON AND R. MATHON, *Int. J. Numer. Methods Eng.* **14**, 1739 (1979).
20. R. L. JOHNSTON AND G. FAIRWEATHER, *Appl. Math. Modelling* **8**, 265 (1984).
21. A. KARAGEORGHIS, D. Phil. thesis, Oxford University, 1984.
22. M. A. KELMANSON, *Comput. Fluids* **11**, 307 (1983).
23. M. A. KELMANSON, *J. Comput. Phys.* **51**, 139 (1983).
24. M. KESHAVARZI, *Comput. Methods Appl. Mech. Eng.* **16**, 1 (1978).
25. V. D. KUPRADZE, *Potential Methods in the Theory of Elasticity* (Israel Program for Scientific Translations, Jerusalem, 1965).
26. V. D. KUPRADZE, *Russian Math. Surveys* **22**, 58 (1967).
27. V. D. KUPRADZE AND M. A. ALEKSIDZE, *U.S.S.R. Comput Math. Math. Phys.* **4**, No. 4, 82 (1964).
28. M. MACDONELL, M. S. thesis, Department of Computer Science, University of Toronto, 1985.
29. M. MAITI AND S. K. CHAKRABARTI, *Int. J. Eng. Sci.* **12**, 793 (1974).
30. R. MATHON, Ph.D. thesis, Department of Computer Science, University of Toronto, 1972.
31. R. MATHON AND R. L. JOHNSTON, *SIAM J. Numer. Anal.* **14**, 638 (1977).
32. S. MURASHIMA, Y. NONAKA, AND H. NIEDA, in *Boundary Elements, Proceedings of the Fifth International Conference, Hiroshima, Japan, 1983*, edited by C. A. Brebbia, T. Futagami, and M. Tanaka (Springer-Verlag, New York, 1983), p. 75.
33. E. R. OLIVEIRA, *J. Eng. Mech. Div., Proc. ASCE* **94**, 79 (1968).
34. G. R. RICHTER, in *Advances in Computer Methods for Partial Differential Equations—II*, edited by R. Vichnevetsky (IMACS (AICA), 1977), p. 41.
35. C. M. SEGEDIN AND D. G. A. BRICKELL, *J. Str. Div. Proc. ASCE* **94**, 41 (1968).
36. M. STERN, *Int. J. Solids and Structures* **15**, 769 (1979).
37. G. T. SYMM, Report NAC 31, National Physical Laboratory, 1973.
38. S. TIMOSHENKO AND S. WOINOWSKY-KRIEGER, *Theory of Plates and Shells* (McGraw–Hill, New York, 1959).
39. H. TOTTENHAM, in *Developments in Boundary Element Methods-1*, edited by P. K. Banerjee and R. Butterfield (Applied Science, London, 1979), p. 173.

40. B. C. Wu and N. J. Altiero, *Comput. Structures* **10**, 703 (1979).
41. R. D. Bhargava, *Proc. Nat. Inst. Sci. India* **31***A*, 571 (1965).
42. P. K. Bhattacharyya and G. T. Symm, *Comput. Math. Appl.* **6**, 443 (1980).
43. P. K. Bhattacharyya and G. T. Symm, *Appl. Math. Modelling* **8**, 226 (1984).
44. D. Redekop, *Appl. Math. Modelling* **6**, 390 (1982).
45. D. Redekop and J. C. Thompson, *Comput. & Structures* **17**, 485 (1983).
46. F. Paris and S. De León, *Int. J. Numer. Methods Eng.* **23**, 173 (1986).